

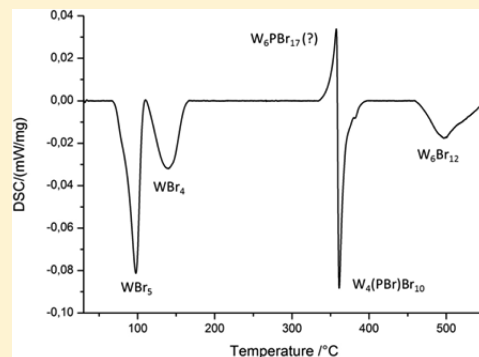
Cluster Harvesting in the WBr_6 -P System

Markus Ströbele, Klaus Eichele, and Hans-Jürgen Meyer*

Section of Solid State and Theoretical Inorganic Chemistry, Institute of Inorganic Chemistry, Eberhard Karls University Tübingen, Auf der Morgenstelle 18, D-72076 Tübingen, Germany

Supporting Information

ABSTRACT: A combined thermal scanning-X-ray diffraction (XRD) approach was performed for the WBr_6 -P system to detect and analyze phases in this system, including metal-rich phases generated with increasing amounts of elemental (red) phosphorus under partial PBr_3 release. Phases were characterized by powder XRD. A black crystalline powder of $W_4(PBr)Br_{10}$ was obtained after reduction of WBr_6 with elemental phosphorus at 450 °C. The crystal structure of the new compound was found to be isotypic with the structure of $W_4(PCI)Cl_{10}$ on the basis of powder XRD data. The structure of $W_4(PBr)Br_{10}$ is represented by a cyclobutadiene-like tetranuclear tungsten cluster interconnected into a layered $(W_4(\mu_4-PBr)Br_6^i)Br_{8/2}^{a-a}$ arrangement via outer bromide ligands. The μ_4 -capping bromophosphinidene ligand was verified by solid-state magic-angle spinning ^{31}P NMR spectroscopy.



INTRODUCTION

A thermal scanning approach has been developed to detect phases with limited thermal stability that are usually hard to find by straightforward solid-state reactions. This approach involves the in situ detection of thermal effects caused by the formation of compounds by means of differential thermal analysis or differential scanning calorimetry (DSC) during heating of a reaction mixture. At the same time, a concentration gradient is implemented in the reaction by using an excess of one reaction partner, which in this case is a reducing agent, to generate metal-rich compounds.

This thermal scanning approach has been successfully employed to detect numerous compounds in the M - W - Cl system with $M = Fe$,¹ Co ,² and Mn ,³ and phases in the Sb - W - Br system.^{1,4}

Recently, the reduction of WCl_6 with phosphorus in a fused-silica tube yielded the new compounds W_6PCI_{17} and $W_4(PCI)Cl_{10}$,⁵ of which the first compound represents a new type of hexanuclear phosphorus-centered W_6 cluster, which can be considered as a structural intermediate between the (empty) W_6Cl_{18} ,⁶ and the carbon-centered W_6CCl_{18} -type cluster.⁷ The discovery of W_6PCI_{17} was indeed guided by serendipity (and persistence) because its thermal stability range (under the reaction conditions used) is approximately between 410 °C (formation) and 440 °C (decomposition). This example clearly emphasizes that phases that exist in a similarly small temperature window can be regarded as undiscovered in most cases of classical solid-state synthesis. The thermal scanning approach was not applied to the P - W - Cl system because the reactivity and pressure of the coproduced PCl_3 offer a serious stability challenge to most container materials.

Meanwhile, we have introduced gold-plated steel as a robust and pressure-resistant container material. Hence, the investigation of the P - W - Br system, which is reported in this

contribution, was explored by the thermal scanning method. Phases appearing during this study were characterized by powder X-ray diffraction (XRD), and the presence of phosphorus in one compound was verified by magic-angle-spinning (MAS) ^{31}P NMR spectroscopy.

RESULTS AND DISCUSSION

The P - W - Br system was investigated for a mixture of WBr_6 and red phosphorus, charged into a modified gold-plated DSC sample holder. The amount of reacting agents was balanced according to reaction (1) to allow the successive reduction of tungsten from W^{VI} to W^{II} sequentially with oxidation stages in between.



A total of five thermal effects were obtained in the DSC measurement during heating of the mixture from room temperature to 550 °C at a rate of 2 K/min (Figure 1). The reaction container remained intact in spite of the significant pressure caused by the increasing formation of PBr_3 . In the following process, separate reactions were performed and assigned to each single thermal effect. Reaction products were inspected by powder XRD, with the corresponding powder XRD patterns displayed in Figure 2. The first and second thermal effects in the DSC measurement were assigned to the formation of WBr_5 and WBr_4 . No known compound could be assigned to the endothermic effect near 350 °C. The exothermic effect above 350 °C was due to the new $W_4(PBr)Br_{10}$ compound, whose structure was refined on the

Special Issue: To Honor the Memory of Prof. John D. Corbett

Received: September 29, 2014

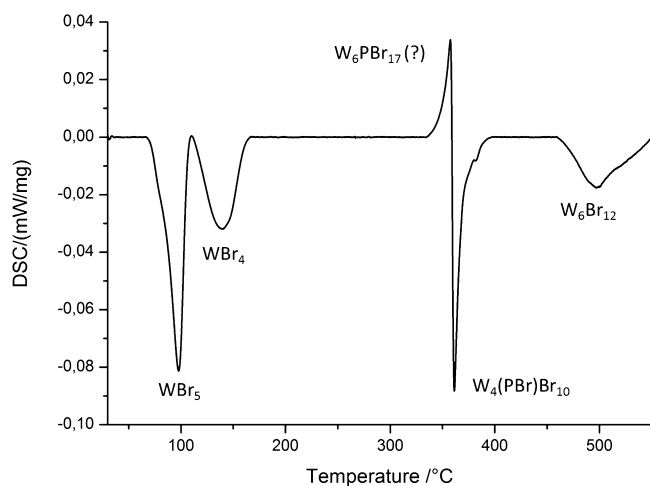


Figure 1. DSC of the successive reduction of WBr_6 with elemental phosphorus powder with increasing temperature (corrected for background).

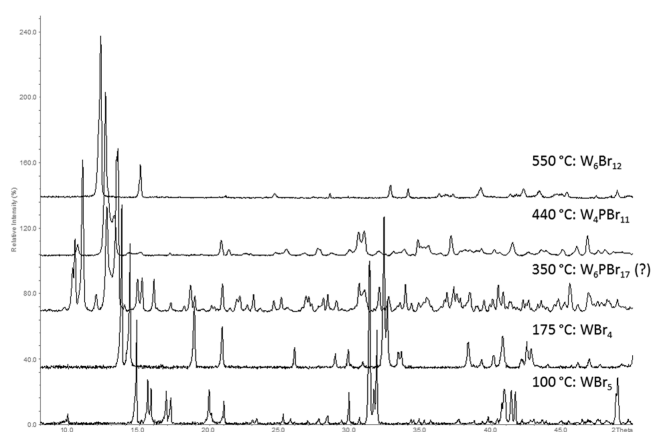


Figure 2. Powder XRD patterns of compounds obtained during the reduction of WBr_6 with elemental phosphorus powder at certain reaction temperatures (given in the figure).

basis of the powder XRD pattern. Finally, the known compound W_6Br_{12} was formed, beginning at about 450 °C (onset).

Compared to the P–W–Cl system, the endothermic effect near 350 °C was expected to relate to formation of the unknown $\text{W}_6\text{PBr}_{17}$. However, the XRD pattern obtained from a reaction with this composition (Figure 2) could not be related to the corresponding XRD pattern of $\text{W}_6\text{PBr}_{17}$ or to any other known tungsten bromide compound.

A comparative DSC study performed in the P–W–Cl system revealed a pattern similar to that with the formation of WCl_5 and WCl_4 in the lower-temperature regime, below 200 °C. At higher temperatures, two endothermic and two exothermic effects were obtained, most likely related to the formation of PCl_3 adducts of $\text{W}_6\text{PBr}_{17}$ (adduct onset at 375 °C; $\text{W}_6\text{PBr}_{17}$ onset at 410 °C) and $\text{W}_4(\text{PBr})\text{Cl}_{10}$ (adduct onset at 450 °C; $\text{W}_4(\text{PBr})\text{Cl}_{10}$ onset at 480 °C). A behavior similar to that with adduct formation has been seen in the course of the reduction of WBr_6 with elemental antimony (e.g., $\text{W}_4\text{Br}_{10}\cdot 2\text{SbBr}_3$ before W_4Br_{10} formation).⁸

With our thermal scanning approach, we demonstrate the detection of an endothermic compound that only exists within

a temperature interval of about 30 °C, although the structure remains unknown up to now.

The crystal structure of $\text{W}_4(\text{PBr})\text{Br}_{10}$, as refined on the basis of powder XRD data, appears to be isotopic to the structure of $\text{W}_4(\text{PCl})\text{Cl}_{10}$. The basic cluster features a Jahn–Teller-distorted rectangular W_4 core following the motif of the butadiene structure (Figure 3). The distances between tungsten atoms

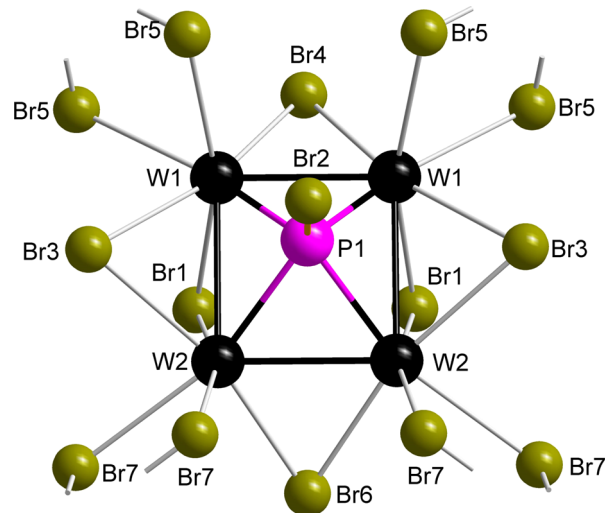


Figure 3. Building block of $(\text{W}_4(\mu_4\text{-PBr})\text{Br}_6)\text{Br}_{8/2}^{2-}$ with atom labels. Br^{a-a} ligands, bridging between adjacent clusters, are indicated with bond sticks.

involve short contacts, $d_{\text{W1}-\text{W1}} = 2.649(3)$ and $d_{\text{W2}-\text{W2}} = 2.665(4)$ Å, and long contacts of $2 \times 2.855(4)$ Å for the $\text{W1}-\text{W2}$ bonds. These distances are slightly (on average 0.038 and 0.046 Å) longer than those in the corresponding chloride compound. Nearest intercluster contacts within layers of $(\text{W}_4(\mu_4\text{-PBr})\text{Br}_6)\text{Br}_{8/2}^{2-}$ are established via bridging Br^{a-a} ligands and involve $\text{W}-\text{W}$ distances of 4.031(4) and 4.048(4) Å. The average $\text{W}-\text{Br}$ distance with bridging Br^{a-a} and Br^{7-a} ligands is 2.649 Å, and that with terminal Br^f is 2.575 Å.

Following this connectivity pattern, the rectangular clusters are interconnected by bridging bromide ligands into a 4^4 layer structure displayed in Figure 4. Alternating layers are linked by van der Waals attractions, whereupon empty rectangular spaces within one layer are stuffed by bromophosphinidene ligands of adjacent layers.

The most remarkable feature of $\text{W}_4(\text{PBr})\text{Br}_{10}$ is the presence of the μ_4 -capping bromophosphinidene ligand, having $\text{W}-\text{P}$ distances of 2.448(8) and 2.466(8) Å and a $\text{P}-\text{Br}$ distance of 2.09(1) Å, which is shorter than the reported $\text{P}-\text{Br}$ distance in PBr_3 [2.212(3)–2.216(4) Å]. This finding is in agreement with the result of the NMR measurement.

In the MAS ^{31}P NMR spectrum of a powder sample of $\text{W}_4(\text{PBr})\text{Br}_{10}$ (Figure 5), direct dipolar and indirect spin–spin coupling interactions with the spin $3/2$ isotopes ^{79}Br and ^{81}Br result in characteristic nonsymmetric multiplets^{9,10} centered at an isotropic chemical shift of 345.7 ppm. The observed splitting can be simulated¹¹ using the following parameters for the $^{79}\text{Br}-^{31}\text{P}$ isotopomer: a direct dipole–dipole coupling constant of 1320 Hz (close to the value calculated from the $\text{P}-\text{Br}$ distance, 1340 Hz), an indirect spin–spin coupling constant of –500 Hz, and a ^{79}Br nuclear quadrupole coupling constant of 250 MHz. The asymmetry parameter of the electric field

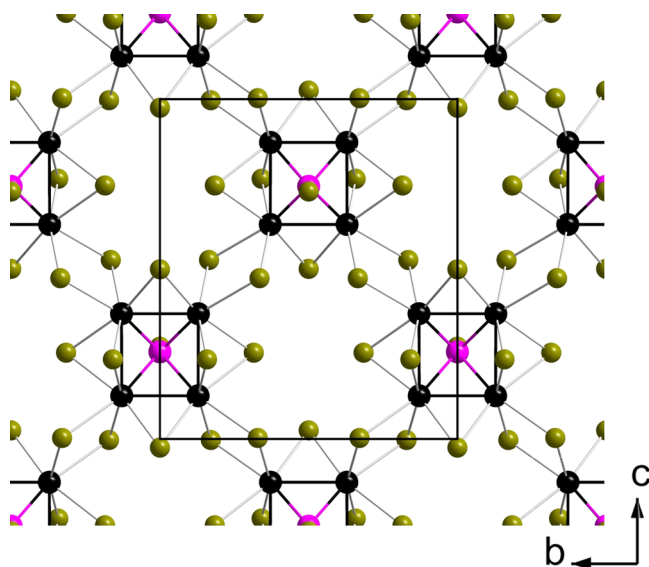


Figure 4. Projection of one layer of the crystal structure of $(W_4(\mu_4\text{-PBr})\text{Br}_6)\text{Br}_{8/2}$.

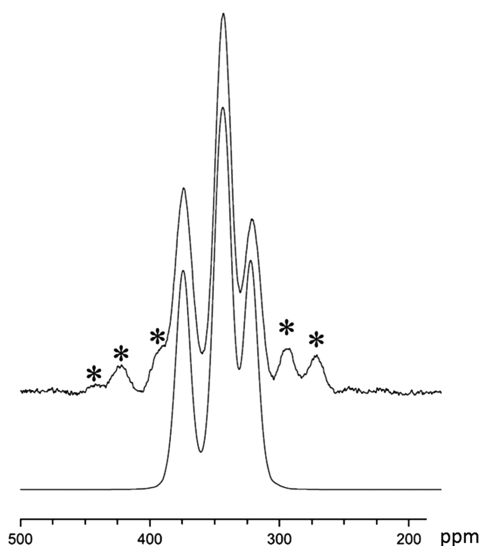


Figure 5. MAS ^{31}P NMR spectrum of $W_4(\text{PBr})\text{Br}_{10}$ including spinning sidebands (*, top) and the calculated spectrum including coupling interactions of ^{31}P with $^{79/81}\text{Br}$ (bottom).

gradient about bromine has been assumed to be zero. The corresponding values of the $^{81}\text{Br}\text{-}^{31}\text{P}$ isotopomer have been calculated by taking into account the magnetogyric ratios, $\gamma(^{81}\text{Br})/\gamma(^{79}\text{Br}) = 1.077$, or the ratios of the nuclear quadrupole moments, $Q(^{81}\text{Br})/Q(^{79}\text{Br}) = 0.8355$. In summary, the multiplet structure observed in the MAS ^{31}P NMR spectrum corroborates the presence of one bromine atom bonded to phosphorus at a relatively short distance. Because of the great line widths, ca. 1 kHz, in the MAS ^{31}P NMR spectrum, satellites due to coupling with ^{183}W (spin $-1/2$, n.a. 14.3%) cannot be resolved.

EXPERIMENTAL SECTION

DSC. A mixture of $W\text{Br}_6$ and elemental red phosphorus (Alfa Aesar, 99%) was combined in a molar ratio corresponding to the composition $W_6\text{Br}_{12}$ (plus the corresponding PBr_3) to allow successive reduction of tungsten from oxidation state 6+ to 2+. The starting mixture (39.6 mg) was loaded under a dry argon atmosphere

(glovebox) into a gold-plated steel container ($V = 100 \mu\text{L}$; Fa. Bächler Feintech, CH) and sealed with a gold plate (99.99% gold). The loaded sample holder and a reference container were inserted into a differential thermal analyzer (STA 204 F1 Phoenix, Fa. Netzsch) and heated at a rate of $2 \text{ }^\circ\text{C}/\text{min}$, while the thermal effects of the progressive reduction steps were monitored.

Preparation of Single Compounds. Compounds were prepared from $W\text{Br}_6$ (300 mg, 0.452 mmol) and elemental red phosphorus (18.7 mg, 0.6 mmol; Alfa Aesar, 99%), which were mixed under an argon atmosphere (glovebox), sealed in an evacuated silica tube, and then heated in a tube furnace (heating and cooling rate of $2 \text{ K}/\text{min}$). The temperature and duration of the reactions were optimized to obtain a high X-ray purity for each compound, leading to the following conditions: $W\text{Br}_5$, 5 min at $100 \text{ }^\circ\text{C}$, black powder; $W\text{Br}_4$, 30 min at $175 \text{ }^\circ\text{C}$, dark-brown powder; unknown compound ($W_6\text{PBr}_{17}$), 9 h at $335 \text{ }^\circ\text{C}$, black powder; $W_4(\text{PBr})\text{Br}_{10}$, 72 h at $450 \text{ }^\circ\text{C}$, dark-green powder; $W_6\text{Br}_{12}$, 72 h at $500 \text{ }^\circ\text{C}$, dark powder.

An excess of elemental phosphorus, which is X-ray amorphous, was present in all reaction products, except for the product targeting the synthesis of $W_6\text{Br}_{12}$. Coproduced PBr_3 was separated by sublimation.

Powder XRD: $W_4(\text{PBr})\text{Br}_{10}$, $M_r = 1645.3 \text{ g}/\text{mol}$, monoclinic space group $C2/m$ (No. 12), $a = 14.0933(3) \text{ \AA}$, $b = 10.3228(2) \text{ \AA}$, $c = 11.8169(2) \text{ \AA}$, $\beta = 93.906(3)^\circ$, $V = 1715.17(6) \text{ \AA}^3$, $Z = 4$, $\rho_{\text{calcd}} = 6.37131 \text{ g}/\text{cm}^3$, θ range = $2.5\text{--}50^\circ$, $\text{Cu K}\alpha_1$ ($\lambda = 1.54060 \text{ \AA}$), $T = 293(2) \text{ K}$, 1020 measured data (STOE StadIP), structure refinement by global refinement (*FullProf Suite*), refined parameters 47, final R indices of $R_p = 0.042$, $R_{\text{wp}} = 0.0565$, $R_{\text{Bragg}} = 0.0409$, and $\chi^2 = 1.345$.

Solid-State NMR. Solid-state MAS ^{31}P NMR spectra were acquired at 4.7 T using a Bruker DSX-200 super-wide-bore spectrometer equipped with a double-bearing broad-band cross-polarization/MAS probe head, operating at 81.01 MHz for ^{31}P NMR. A powdered sample was packed into a 4 mm (o.d.) zirconia rotor sealed with a Kel-F cap. Spectra were acquired after single-pulse excitation with a spinning frequency of 4 kHz, a recycle delay of 30 s, and 2406 scans. ^{31}P chemical shifts are reported with respect to external 85% aqueous phosphoric acid. Spectral simulations were carried out using *WSolids1*.¹¹

CONCLUSION

A combined thermal scanning–XRD approach has shown several phases in the P–W–Br system and their stability ranges under given conditions. On this basis, the new compound $W_4(\text{PBr})\text{Br}_{10}$ was separately prepared and structurally characterized. The crystal structure is isotypic with $W_4(\text{PCl})\text{Cl}_{10}$ and comprises a bromophosphinidene-capped tungsten cluster, as refined from powder XRD data and confirmed by MAS ^{31}P NMR spectra. The compound appears quite stable in air and water, showing an unchanged powder XRD pattern after exposure to air for 1 week.

Thermal scanning–XRD has shown once more its capability to detect and subsequently prepare thermally labile cluster moieties with no more than six cluster atoms (*the missing children in cluster chemistry*). An expansion of this methodology to other metal halides that are known from cluster compounds is likely.

ASSOCIATED CONTENT

Supporting Information

X-ray crystallographic information for $W_4(\text{PBr})\text{Br}_{10}$ in CIF format. This material is available free of charge via the Internet at <http://pubs.acs.org>.

AUTHOR INFORMATION

Corresponding Author

*E-mail: juergen.meyer@uni-tuebingen.de.

Notes

The authors declare no competing financial interest.

■ REFERENCES

- (1) Ströbele, M.; Mos, A.; Meyer, H.-J. *Inorg. Chem.* **2013**, *52*, 6951–6956.
- (2) Mos, A.; Ströbele, M.; Meyer, H.-J. *J. Cluster Chem.* **2014**.
- (3) Mos, A.; Ströbele, M.; Meyer, H.-J. In preparation.
- (4) Ströbele, M.; Meyer, H.-J. *Z. Anorg. Allg. Chem.* **2012**, *638* (6), 945–949.
- (5) Ströbele, M.; Eichele, K.; Meyer, H.-J. *Eur. J. Inorg. Chem.* **2011**, *26*, 4063–4068.
- (6) Siepman, R.; von Schnering, H. G.; Schäfer, H. *Angew. Chem.* **1967**, *79*, 650. Nägele, A.; Glaser, J.; Meyer, H.-J. *Z. Anorg. Allg. Chem.* **2001**, *627*, 244–249.
- (7) Zheng, Y.-Q.; von Schnering, H. G.; Chang, J. H.; Grin, Y.; Engelhardt, G.; Heckmann, G. *Z. Anorg. Allg. Chem.* **2003**, *629*, 1256–1264.
- (8) Ströbele, M.; Meyer, H.-J. *Russ. J. Coord. Chem.* **2012**, *38* (3), 178–182.
- (9) Rabis, A.; Grimmer, A.-R.; Thomas, B.; Brendler, E.; Beck, S.; Meisel, M. *Solid State Nucl. Magn. Reson.* **2005**, *28*, 57–63.
- (10) Thomas, B.; Paasch, S.; Steuernagel, S.; Eichele, K. *Solid State Nucl. Magn. Reson.* **2001**, *20*, 108–117.
- (11) Eichele, K. *WSolids1*, version 1.20.21; Universität Tübingen: Tübingen, Germany, 2013.